Central European Journal of Energetic Materials
ISSN 1733-7178; e-ISSN 2353-1843

Cent. Eur. J. Energ. Mater. 2018, *15*(1): 85-99; DOI: 10.22211/cejem/81082

Synthesis, Characterization and Compatibility Studies of Poly(DFAMO/NIMMO) with Propellant and PBX Ingredients

Huan Li,[1*] Yifei Yang,[1] Jiaan Pan,[1] Wanjun Wang,[1,2] Renming Pan,[1] Weihua Zhu[1]

[1] *School of Chemical Engineering, Nanjing University of Science and Technology, 200 Xiao Lingwei, 210094 Nanjing, China*
[2] *Shanghai Institute of Organic Chemistry, Chinese Academy of Sciences, China*
[*] *E-mail: lihuannjust@163.com*

Abstract: Oxetane-based polymers substituted with difluoroamino groups can be used as energetic binders in propellants and polymer-bonded explosives (PBXs). As a novel candidate, poly(3-difluoroaminomethyl-3-methyloxetane/3-nitratomethyl-3-methyloxetane) (PDN) was synthesized and its structure was established. Thermogravimetry (TG) and differential scanning calorimetry (DSC) were employed to investigate its thermal decomposition behaviour. The compatibility between PDN and some common ingredients of propellants and PBXs was evaluated by the DSC method. PDN with good thermal stability was synthesized *via* a cationic solution polymerization process. Additionally, it has improved compatibility with cyclotetramethylenetetranitramine (HMX), carbon black (C.B.) and lead carbonate ($PbCO_3$) compared with homopoly(3-difluoroaminomethyl-3-methyloxetane) (PDFAMO). PDN could be used as a promising difluoroamino energetic binder in the future.

Keywords: energetic binder, synthesis, characterization, compatibility, PDN

1 Introduction

Containing both difluoroamino and nitrate ester groups, poly(3-difluoroaminomethyl-3-methyloxetane/3-nitratomethyl-3-methyloxetane) (PDN) can be used as an energetic pre-polymer in energetic binder systems of propellants

and polymer-bonded explosives. Little research about this energetic co-polymer has been reported before. However there are some works that focused on the polymerization process, the structure characterization and properties of homo- and co-polymers of 3-difluoroaminomethyl-3-methyloxetane (DFAMO) [1-5] and 3-nitratomethyl-3-methyloxetane (NIMMO) [6-10]. Their controllable structures, good thermal properties and low glass transition temperatures have increased their possible practical use. By combining the DFAMO and NIMMO segments in one polymer chain, PDN is designed as a new kind of energetic polymer.

Meanwhile, the compatibility between this new energetic material and the contacted components in propellants and PBXs represents an important phase in the pre-formulation stage for the development of all new energetic forms [11]. The contacted components should be compatible with each other in order to ensure the safe storage and use of the propellants and PBXs [12]. Thermoanalytical methods are sufficiently sensitive to give an early indication of incipient chemical decomposition or chemical reaction, *i.e.* stability and incompatibility [13]. In addition, the DSC method can provide compatibility results that are similar to vacuum stability test results for the same combinations [14]. Various works have been done on the compatibility of oxetane-based energetic polymers with contacted materials by the DSC method [15-18]. In order to achieve at a better understanding of the relationship between the structure and reactivity of these oxetane-based difluoroamino polymers, this paper focuses on the synthesis, characterization and compatibility of PDN with some ingredients which are commonly used in propellants and PBXs, using the DSC method.

2 Materials and Methods

2.1 Materials

*2.1.1 Synthesis of PDN (**1**)*

DFAMO was synthesized and purified *via* Manser's method [1, 2]. NIMMO was synthesized by directly nitrating 3-hydroxymethyl-3-methyloxetane under non-acidic anhydrous conditions [19]. Butanediol (BDO), boron trifluoride etherate (TFBE) and 1,2-dichloroethane were distilled under vacuum before use. BDO and TFBE were used as the initiator and catalyst during the polymerization process. The cationic polymerization process of DFAMO and NIMMO was performed in 1,2-dichloroethane. All glassware was pre-dried and purged with dry nitrogen before the introduction of the reactants. 1,2-Dichloroethane (15.0 mL) and BDO (0.27 mL, 3.0 mmol) were added to a 50 mL flask equipped

with magnetic stirrer under a nitrogen atmosphere, followed by TFBE (0.192 mL, 1.5 mmol). The solution was stirred for 1 h at room temperature and then cooled to 0 °C. After 30 min, a solution of DFAMO (5.00 g, 0.036 mol), NIMMO (5.36 g, 0.036 mol) in 1,2-dichloroethane (15.0 mL) was slowly injected into the flask during 0.5 h. The reaction was quenched by the injection of a saturated solution of $NaHCO_3$ in water (5 mL) after 24 h. The organic layer was separated, washed with a saturated aqueous solution of NaCl, dried over sodium sulfate, and evaporated to dryness. The total yield was 80%. The copolymer was then washed 3 times with cold methanol (3×100 mL) to remove the oligomers and dried at 50 °C under vacuum for 12 h before testing.

GPC: M_n=7091, M_w=9712, M_w/M_n=1.37. ^{1}H NMR (400 MHz, $CDCl_3$, 25 °C): δ 0.97 (s, 3H, CH_3 in NIMMO segments), 1.00 (s, 3H, CH_3 in DFAMO segments), 3.25 (m, 4H, OCH_2), 3.47 (t, 2H, CH_2NF_2), 4.36 ppm (s, 2H, CH_2ONO_2). ^{19}F NMR ($CDCl_3$): δ 64.29 ppm (m, NF_2). ^{13}C NMR ($CDCl_3$): δ 17.20 (s, CH_3 in NIMMO segments), 18.41 (s, CH_3 in DFAMO segments), 26.19 (d, CH_2 in BDO segments), 39.62 (t, quaternary carbon in DFAMO segments), 40.31 (s, quaternary carbon in NIMMO segments), 68.92 (s, CH_2NF_2), 73.46 (m, OCH_2), 74.91 ppm (s, CH_2ONO_2). FTIR: ν(C-N) 802, ν(O-N) 856, ν(N-F) 895, ν(C-O) 972, ν(C-O) 985, ν(N-F) 1046, ν(C-O-C) 1103, ν_s(NO_2) 1277, ν(C-H) 1366, ν(C-H) 1463, ν_{as}(NO_2) 1626, ν(NF_2) 1738, ν(C-H) 2878, ν(C-H) 2971 cm^{-1}. Elemental analysis: $C_{249.95}H_{452.71}O_{127.81}N_{49.19}F_{47.3}$ (7090.88); C 42.67 (calc. 42.34); H 6.49 (6.44); N 9.57 (9.72); F 12.64 (12.67) %. Functionality: 2.01. Glass transition temperature: −25.5 °C.

2.1.2 Preparation of single and mixed systems for compatibility evaluation

Single systems were separated into four types and all of the materials were pre-dried at 55 °C for 1 day before use.

(a) Explosives. Cyclotrimethylenetrinitramine (RDX (**2**)) (>99.6%), HMX (**4**) (>99.5%), hexanitrohexaazaisowurtzitane (CL-20 (**6**)) (>99.7%), nitroguanidine (NQ (**8**)) (>99.0%), 2,4,6-trinitrotoluene (TNT (**10**)) (>99.5%) 1,3,5-triamino-2,4,6-trinitrobenzene (TATB (**12**)) (>99.5%), pentaerythritol tetranitrate (PETN (**14**)) (>99.5%) and nitrocellulose (NC (**16**)) (ω_N=12.0%).

(b) Oxidizers. Ammonium chlorate(VII) (AP (**18**)) (>99.0%), ammonium nitrate(V) (AN (**20**)) (>99.0%) and potassium nitrate(V) (KNO_3 (**22**)) (>99.0%).

(c) Metal powders. Aluminum powder (Al (**24**)) (particle size = 1-3 μm, >99.95%), magnesium powder (Mg (**26**)) (particle size = 74 μm, >99.0%) and boron powder (B (**28**)) (particle size = 10-20 μm, >99.99%).

(d) Centralites and other inert additives. Diphenylamine (DPA (**30**)) (>99.0%), p-nitro-*N*-methylaniline (PNMA (**32**)) (>98.0%), 2-nitrodiphenylamine (NDPA (**34**)) (>98.0%), 1,3-diethyl-1,3-diphenylurea (C_1 (**36**)) (>99.0%), C.B. (**38**) (>99.9%), aluminum oxide (Al_2O_3 (**40**)) (particle size = 5-6 μm, >99.99%) and $PbCO_3$ (**42**) (>99.99%).

The mixed systems were weighed and mixed systematically in acetone with mass ratios of 1:1. All samples were then dried at 55 °C for 2 days before use. They are listed in the following order. RDX/PDN (**3**), HMX/PDN (**5**), CL-20/PDN (**7**), NQ/PDN (**9**), TNT/PDN (**11**), TATB/PDN (**13**), PETN/PDN (**15**), NC/PDN (**17**), AP/PDN (**19**), AN/PDN (**21**), KNO_3/PDN (**23**), Al/PDN (**25**), Mg/PDN (**27**), B/PDN (**29**), DPA/PDN (**31**), PNMA/PDN (**33**), NDPA/PDN (**35**), C_1/PDN (**37**), C.B./PDN (**39**), Al_2O_3/PDN (**41**), $PbCO_3$/PDN (**43**).

2.2 Thermal and non-thermal techniques

2.2.1 Thermal techniques

DSC: (a) The glass transition temperature was measured using a TA DSC Q2000. The sample of weight ~4-5 mg was initially cooled from room temperature to −70 °C, heated to 70 °C, then cooled and rescanned again from −70 °C to 70 °C. Samples were sealed in aluminum crucibles (100 μL); the heating and cooling rates were 20 °C·min^{-1} under a constant flow of nitrogen (50 mL·min^{-1}). (b) The compatibility evaluation was carried out using a Mettler-Toledo DSC823e. Each sample weighed 0.50-0.60 mg and was sealed in an aluminum crucible (40 μL) with a perforated cover under a constant flow of nitrogen (30 mL·min^{-1}). The heating range and heating rate were 50-500 °C and 10 °C·min^{-1}, respectively.

TG: TG analyses were performed on a Metler-Toledo TGA/SDTA851e, scanning from 50 °C to 500 °C at a heating rate of 10 °C·min^{-1}. The samples were contained in alumina crucibles (70 μL) under a constant flow of nitrogen (30 mL·min^{-1}).

2.2.2 Non-thermal techniques

Nuclear magnetic resonance (NMR): An Agilent 400 MHz instrument was used to measure the ^{1}H, ^{19}F and ^{13}C NMR spectra in chloroform-d.

Gel permeation chromatography (GPC): GPC analyses were recorded on a Waters instrument fitted with a 2414 differential reflective index detector, against polystyrene standards using tetrahydrofuran as eluent at 1 mL·min^{-1}.

Fourier transform infrared spectroscopy (FTIR): FTIR spectra were measured using a Nicolet iS10 instrument.

Elemental analysis: The C, H and N contents were recorded on a Elementar Vario EL III instrument, and the F content was measured with a Metrohm 905 Titrando instrument.

Functionality: Functionality was measured and calculated *via* a ^{1}H NMR method [20-21].

2.3 Compatibility evaluation standards for the DSC method

Table 1 lists the evaluated standards of compatibility for explosive and contacted materials using the DSC method [22].

Table 1. Evaluated standards of compatibility for explosive and contacted materials

Criteria ΔT_p [°C]	Rating[a]
≤2	A Compatible or good compatibility
3-5	B Slightly sensitized or moderate compatibility
6-15	C Sensitized or poor compatibility
>15	D Hazardous or bad compatibility

[a] A: safe for use in any explosive design; B: safe for use in testing, when the device will be used in a very short period of time, not to be used as a binder material, or when long-term storage is desired; C: not recommended for use with explosive items; D: hazardous, do not use under any conditions.

3 Results and Discussion

3.1 Structure characterization and thermal decomposition behavior

Figure 1 shows the ^{1}H and ^{13}C NMR spectra of PDN. The peaks at 0.97 ppm and 1.00 ppm are related to the methyl groups in the DFAMO and NIMMO segments, respectively. The methylene groups adjacent to the nitrate groups in the NIMMO segments are responsible for the peak at 4.36 ppm. By calculating these peak areas, the molar ratio of NIMMO and DFAMO was obtained. The peaks near 26 ppm in the ^{13}C NMR spectra belong to the central two methylenes in the BDO segments. The absence of peaks near 30 ppm indicated that all of the BDO segments were located in the middle of the polymer structures [23]. The calculated structure of PDN is presented in Figure 2. The values of the experimental and calculated mass contents of the elements were very close, and also support the suggested structure of PDN.

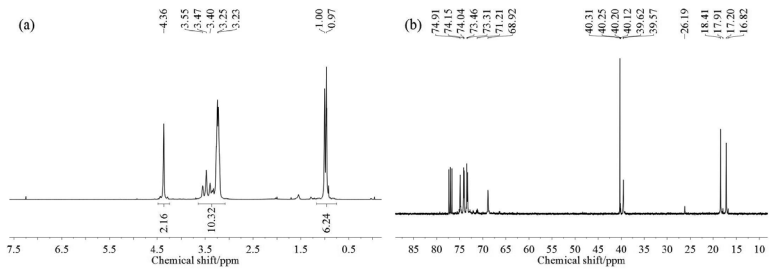

Figure 1. (a) ^{1}H NMR and (b) ^{13}C NMR spectra of PDN

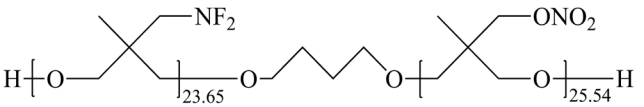

Figure 2. Calculated structure of PDN

Figure 3 presents the TG and DSC curves of PDN. The DSC curve shows only one exothermic peak at 223.7 °C, which is related to the first mass loss in the TG curve, with a mass loss of ~39.5%. This stage could involve the thermal decomposition of the energetic groups (calculated mass content: 41.3%). More works need to be done to determine the specific thermal decomposition mechanism. The second mass loss stage in the TG curve does not relate to the exothermic or endothermic portions of the DSC curve; this was also observed in the earlier reports [10, 24]. About 5.8% mass of residue remained above 450 °C, which may be the extra carbon in the polymer chain. PDN has good thermal stability since it barely decomposes below 180 °C.

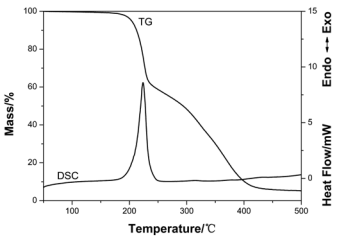

Figure 3. TG and DSC curves of PDN

3.2 Compatibility evaluation

3.2.1 Compatibility of PDN with explosives

Figure 4 presents the typical DSC curves of systems **1-17** and Table 2 lists the compatibility of PDN with some explosives. The data for the DSC curves of single

systems, except for PDN, were obtained from our recent work [5]. The binary system of RDX/PDN had one exothermic peak and the value of ΔT_p between PDN and the RDX/PDN mixture was 1.2 °C, which means that PDN is compatible with RDX. The endothermic peak at 186.3 °C in the HMX/PDN system belongs to melting of HMX. The two separated exothermic peaks at 221.8 °C and 256.0 °C are caused mainly by the separate thermolysis of PDN and HMX. The presence of PDN influences the thermal decomposition of HMX and changes the DSC curve into a smoother and gentler one. The value of ΔT_p between PDN and the HMX/PDN mixture was 1.9 °C, which indicates that this combination can be compatible. The NIMMO segments influence the reactivity of PDN, and cause it to be the first of the oxetane-based difluoroamino polymers to be classified as compatible with HMX by the DSC method. The values of ΔT_p between PDN and the CL-20/PDN and NQ/PDN mixtures were 5.7 °C and 7.5 °C, respectively, which means that these mixtures are sensitized. In addition, both of the values of ΔT_p between PDN and the HMX/PDN and CL-20/PDN systems are obviously lower in comparison with those with PDFAMO. In other words, the NIMMO segments increase the compatibility of PDN with nitramine explosives.

Table 2. Evaluation of compatibility of PDN with explosives from the DSC peak temperature[a]

System		Peak temperature			Rating
Mixed system	Single system	T_{p1} [°C]	T_{p2} [°C]	ΔT_p [°C]	
RDX/PDN (**3**)	PDN (**1**)	223.7	222.5	1.2	A
HMX/PDN (**5**)	PDN (**1**)	223.7	221.8	1.9	A
CL-20/PDN (**7**)	PDN (**1**)	223.7	218.0	5.7	C
NQ/PDN (**9**)	PDN (**1**)	223.7	216.2	7.5	C
TNT/PDN (**11**)	PDN (**1**)	223.7	217.8	5.9	C
TATB/PDN (**13**)	PDN (**1**)	223.7	223.3	0.4	A
PETN/PDN (**15**)	PETN (**14**)	201.5	203.2	−1.7	A
NC/PDN (**17**)	NC (**16**)	208.2	202.2	6.0	C

[a] Mixed system, 1:1-energetic ingredients/PDN binary system; single system, system of pure energetic component, where exothermic peak temperature is the smaller of the two pure ingredients; T_{p1}, the maximum exothermic peak temperature of single system; T_{p2}, the maximum exothermic peak temperature of the mixed system; $\Delta T_p = T_{p1} - T_{p2}$.

The DSC curve of TNT/PDN has a wider exothermic peak, with the peak temperature shifting from 223.7 °C to 217.8 °C. This may not reflect the actual reactivity situation because the endothermic peak of TNT partly overlaps with the exothermic peak of PDN, which may cause errors, and the compatibility of this mixture should be evaluated by other methods for a more accurate result.

TATB did not influence the exothermic thermal decomposition of PDN and the value of ΔT_p between PDN and the TATB/PDN mixture was 0.4 °C.

The endothermic peak at 140.3 °C in the DSC curve of PETN/PDN belongs to the phase change of PETN from solid to liquid. Furthermore the exothermic peak of the mixed system became broader at 203.2 °C. The exothermic peak of NC/PDN moved to 202.2 °C. The values of ΔT_p between PDN and the PETN/PDN and NC/PDN mixtures were −1.7 °C and 6.0 °C respectively, which means PDN is compatible with PETN but sensitized by NC. These differing results could be caused by different thermal decomposition processes of PETN and NC [25-26].

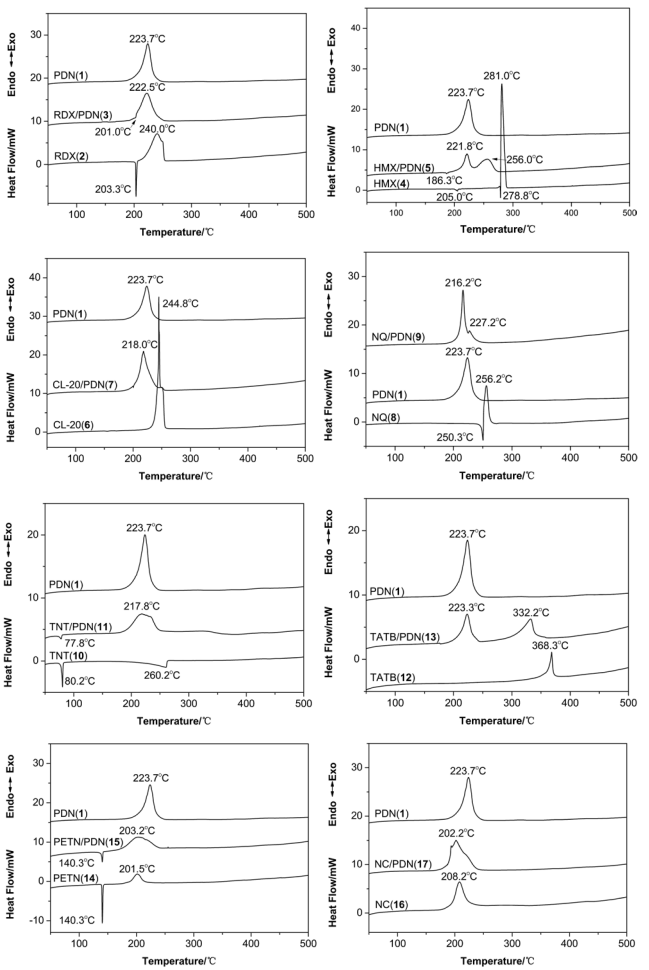

Figure 4. Typical DSC curves of systems **1-17**

3.2.2 Compatibility of PDN with oxidizers

Figure 5 presents the DSC curves of the PDN/oxidizer systems. Table 3 lists the compatibility results. There were two exothermic peaks in the DSC curve of the AP/PDN mixture, which were attributed to PDN and AP individually. The thermal decomposition of PDN was not affected by the presence of AP, and the value of ΔT_p between PDN and AP/PDN was 0.9 °C. The first two endothermic peaks in the DSC curve of AN/PDN are caused by the solid to solid phase transition of AN, and the third endothermic peak is caused by its melting process. The thermolysis processes of AN and PDN overlap to form one exothermic peak in the DSC curve, with a ΔT_p value of 2.7 °C. The DSC curve of KNO_3 had only one endothermic peak, caused by the melting process. The exothermic peak of KNO_3/PDN moved to 228.5 °C, which indicated that KNO_3 and PDN had good compatibility. The second exothermic peak is due to thermolysis of the combination of KNO_3 and polymer residues.

Table 3. Evaluation of compatibility of PDN with oxidizers from the DSC peak temperature

System		Peak temperature			Rating
Mixed system	Single system	T_{p1} [°C]	T_{p2} [°C]	ΔT_p [°C]	
AP/PDN (**19**)	PDN (**1**)	223.7	222.8	0.9	A
AN/PDN (**21**)	PDN (**1**)	223.7	221.0	2.7	B
KNO_3/PDN (**23**)	PDN (**1**)	223.7	228.5	−4.8	A

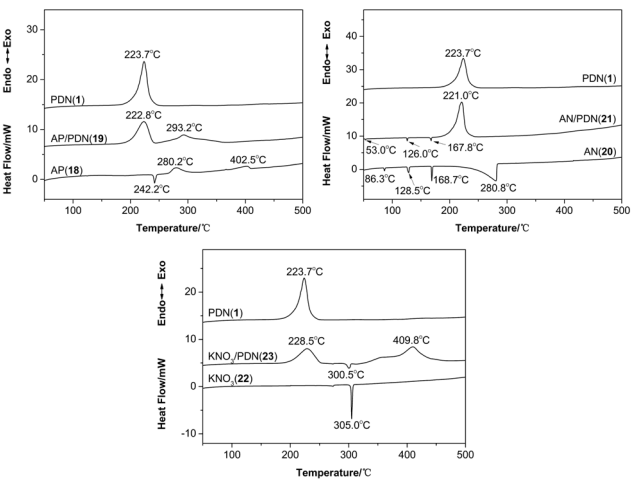

Figure 5. Typical DSC curves of systems **18**-**23**

3.2.3 Compatibility of PDN with metal powders

Figure 6 shows the DSC curves of the thermal decomposition processes of PDN, metal powders and their corresponding mixtures. Table 4 lists the exothermic peak temperatures and compatibility ratings. The presence of Al powder does not apparently change the exothermic peak temperature of PDN, but smooths the shape of the DSC curve. Mg powder does not affect the shape of the exothermic peak, but causes the peak temperature to be decreased by about 2.2 °C. The presence of B influences significantly the thermolysis of PDN. The first peak at 154.5 °C could relate to the thermal decomposition of the difluoroamino groups, while the second one could be the thermal decomposition of the nitrate ester groups. The compatibility of the binary systems with metal powders/PDN decreases in the order: **25**>**27**>**29**.

Table 4. Evaluation of compatibility of PDN with metal powders from the DSC peak temperature

System		Peak temperature			Rating
Mixture system	Single system	T_{p1} [°C]	T_{p2} [°C]	ΔT_p [°C]	
Al/PDN (**25**)	PDN (**1**)	223.7	223.2	0.5	A
Mg/PDN (**27**)	PDN (**1**)	223.7	221.5	2.2	B
B/PDN (**29**)	PDN (**1**)	223.7	154.5	69.2	D

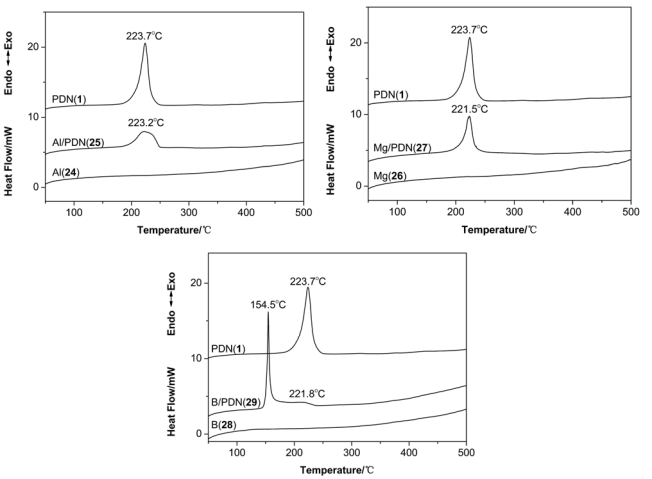

Figure 6. Typical DSC curves of systems **24**-**29**

3.2.4 Compatibility of PDN with Centralites and other inert additives

The typical DSC curves of systems **30**-**43** are shown in Figure 7. Table 5 lists the compatibility of PDN with some Centralites. DPA/PDN has shoulders at 167.8 °C and 219.5 °C. PNMA and NDPA could also affect the thermal decomposition of PDN, with the occurrence of shoulders in the DSC curves. The values of ΔT_p between PDN and DPA/PDN, PNMA/PDN, NDPA/PDN were 55.9 °C, 49.4 °C and 8.2 °C, respectively. Their compatibility decreases in the order: **41**>**39**>**37**. This observation could be caused by differences among the reactivities of the secondary amines. The stronger the steric hindrance and the weaker the alkalinity, the more stable are the secondary amines and the α-Hs of the difluoroamino groups. C_1 does not change the thermal decomposition process of PDN, but only smooths the exothermic process. The value of ΔT_p between PDN and C_1/PDN was −0.3 °C which implies they are compatible.

The presence of C.B., Al_2O_3 and $PbCO_3$ does not obviously change the exothermic peak temperatures of PDN, but only smooth the peak shapes. The values of ΔT_p between PDN and C.B./PDN, Al_2O_3/PDN, $PbCO_3$/PDN were −0.1 °C, −1.1 °C and 0.7 °C, respectively. This indicates that all of these inert additives are safe for use with PDN.

Table 5. Evaluation of compatibility of PDN with Centralites and other inert additives from the DSC peak temperature

System		Peak temperature			Rating
Mixed system	Single system	T_{p1} [°C]	T_{p2} [°C]	ΔT_p [°C]	
DPA/PDN (**31**)	PDN (**1**)	223.7	167.8	55.9	D
PNMA/PDN (**33**)	PDN (**1**)	223.7	174.3	49.4	D
NDPA/PDN (**35**)	PDN (**1**)	223.7	215.5	8.2	C
C_1/PDN (**37**)	PDN (**1**)	223.7	224.0	−0.3	A
C.B./PDN (**39**)	PDN (**1**)	223.7	223.8	−0.1	A
Al_2O_3/PDN (**41**)	PDN (**1**)	223.7	224.8	−1.1	A
$PbCO_3$/PDN (**43**)	PDN (**1**)	223.7	223.0	0.7	A

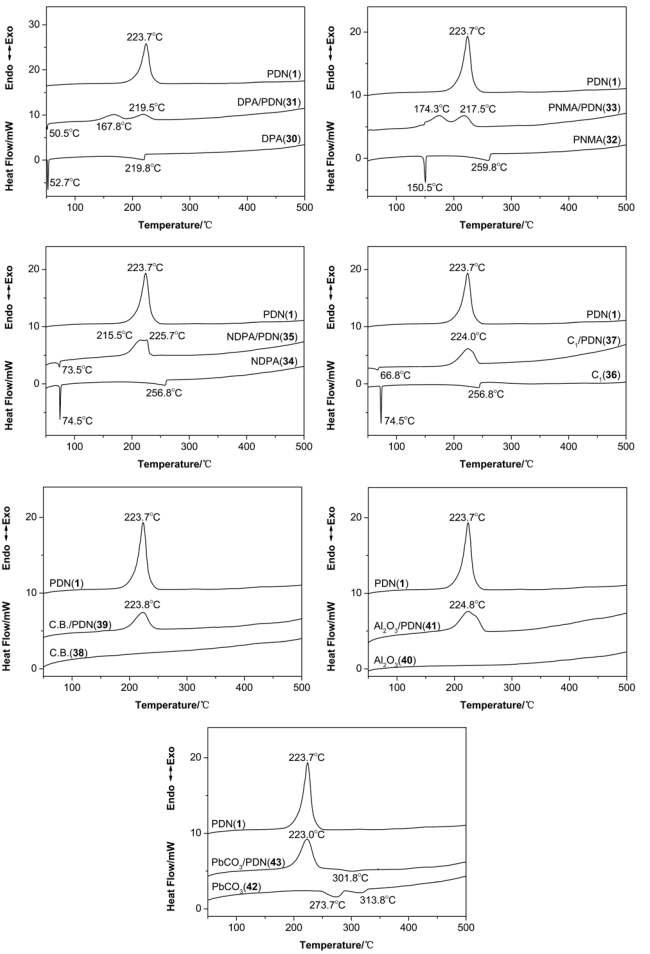

Figure 7. Typical DSC curves of systems **30**-**43**

4 Conclusions

PDN with good thermal stability and low glass transition temperature can be readily synthesized *via* cationic solution polymerization using BDO and TFBE as initiator and catalyst, respectively. The copolymer is monomer-ended, with the BDO segments all located in the middle of the polymer chain. A compatibility study between PDN and some common ingredients of propellants and PBXs has been investigated by the DSC method. PDN is compatible with RDX, HMX,

TATB, PETN, AP, KNO_3, Al, C_1, C.B., Al_2O_3 and $PbCO_3$, is slightly sensitized by AN and Mg, is sensitized by CL-20, NQ, TNT, NC and NDPA, and is hazardous with B, DPA and PNMA, respectively. The compatibility of the mixed systems decreases in the order: **23**>**15**>**41**>**37**>**39**>**13**>**25**>**43**>**19**>**3**>**5**>**27**>**21**>**7**>**11**>**17**>**9**>**35**>**33**>**31**>**29**, while the relative thermal stability decreases in the order: **23**>**41**>**37**>**39**>**13**>**25**>**43**>**19**>**3**>**5**>**27**>**21**>**7**>**11**>**9**>**35**>**15**>**17**>**33**>**31**>**29**. The NIMMO segment improves the compatibility of PDN with HMX, C.B. and $PbCO_3$ by comparison with PDFAMO.

Acknowledgements

This work was supported by the National Natural Science Foundation of China (Grant No. 51603103).

References

[1] Archibald, T. G.; Manser, G. E.; Immoos, J. E. *Difluoroamino Oxetanes and Polymers Formed Therefrom for Use in Energetic Formulations*. Patent US 5272249, **1993**.

[2] Archibald, T. G.; Manser, G. E.; Immoos, J. E. *Difluoroamino Oxetanes and Polymers Formed Therefrom for Use in Energetic Formulations.* Patent US 5420311, **1995**.

[3] Li, H.; Pan, R. M.; Wang, W. J.; Zhang, L. Y. Thermal Decomposition, Kinetics and Compatibility Studies of Poly(3-difluoroaminomethyl-3-methyloxetane) (PDFAMO). *Propellants Explos. Pyrotech.* **2014**, *39*(6): 819-829.

[4] Li, H.; Pan, R. M.; Wang, W. J.; Zhang, L. Y. Thermal Decomposition and Kinetics Studies on Poly(BDFAO/THF), Poly(DFAMO/THF), and Poly(BDFAO/DFAMO/THF). *J. Therm. Anal. Calorim.* **2014**, *118*(1): 189-196.

[5] Li, H.; Pan, J. A.; Wang, W. J.; Pan, R. M.; Zhu, W. H. Preparation, Characterization and Compatibility Studies of Poly(DFAMO/AMMO). *J. Macromol. Sci. Part A Pure Appl. Chem.* **2018**, 55(2):135-141, doi:10.1080/10601325.2017.1387742.

[6] Desai, H. J.; Cunliffe, A. V.; Hamid, J.; Honey, P. J.; Stewart, M. J. Synthesis and Characterization of α,ω-Hydroxy and Nitrato Telechelic Oligomers of 3,3-(Nitratomethyl) Methyl Oxetane (NIMMO) and Glycidyl Nitrate (GLYN). *Polymer* **1996**, *37*(15): 3461-3469.

[7] Kimura, E.; Oyumi, Y.; Kawasaki, H.; Maeda, Y.; Anan, T. Characterization of BAMO/NMMO Copolymers. *Propellants Explos. Pyrotech.* **1994**, *19*(5): 270-275.

[8] Kawasaki, H.; Anan, T.; Kimura, E.; Oyumi, Y. BAMO/NMMO Copolymer with Polyester Initiation. *Propellants Explos. Pyrotech.* **1997**, *22*(2): 87-92.

[9] Akhavan, J.; Koh, E.; Waring, S.; Kronfli, E. Effect of UV and Thermal Radiation on PolyNIMMO. *Polymer* **2001**, *42*(18): 7711-7718.

[10] Chang, H. The Investigation of Thermal Decomposition Kinetics for PNIMMO by TG-MS. (in Chinese) *Initiators Pyrotechnics* **2007**, (2): 32-35.
[11] Li, X.; Wang, B. L.; Lin, Q. H. Compatibility Study of 2,6-Diamino-3,5-dinitropyridine-1-oxide with Some Energetic Materials. *Cent. Eur. J. Energ. Mater.* **2016**, *13*(4): 978-988.
[12] Gołofit, T.; Zysk, K. Thermal Decomposition Properties and Compatibility of CL-20 with Binders HTPB, PBAN, GAP and PolyNIMMO. *J. Therm. Anal. Calorim.* **2015**, *119*(3): 1931-1939.
[13] Agrawal, J. P. *High Energy Materials. Propellants, Explosives and Pyrotechnics.* Wiley-VCH, Germany **2010**, pp. 179; ISBN 978-3-527-32610-5.
[14] Klerk, W. P. C.; Schrader, M. A.; Steen, A. C. Compatibility Testing of Energetic Materials, Which Technique? *J. Therm. Anal. Calorim.* **1999**, *56*(3): 1123-1131.
[15] Song, X. D.; Zhao, F. Q.; Wang, J. N.; Gan, X. X.; Xie, B. Thermal Behaviors of BAMO-AMMO and Its Compatibility with Some Energetic Materials. *Chin. J. Explos. Propellants* **2008**, *31*(3): 75-78.
[16] Liao, L. Q.; Wei, H. J.; Li, J. Z.; Fan, X. Z.; Zheng, Y.; Ji, Y. P.; Fu, X. L.; Zhang, Y. J.; Liu, F. L. Compatibility of PNIMMO with Some Energetic Materials. *J. Therm. Anal. Calorim.* **2012**, *109*(3): 1571-1576.
[17] Pei, J. F.; Zhao, F. Q.; Lu, H. L.; Song, X. D.; Zhou, R.; Yuan, Z. F.; Zhang, J.; Chen, J. B. Compatibility of BAMO-GAP Copolymer with Some Energetic Materials. *J. Therm. Anal. Calorim.* **2016**, *124*(3): 1301-1307.
[18] Shee, S. K.; Shah, P. N.; Athar, J.; Dey, A.; Soman, R. R.; Sikder, A. K.; Pawar, S.; Banerjee, S. Understanding the Compatibility of the Energetic Binder PolyNIMMO with Energetic Plasticizers: Experimental and DFT Studies. *Propellants Explos. Pyrotech.* **2016**, *42*(2): 167-174.
[19] Manser, G. E.; Hajik, R. M. *Method of Synthesizing Nitrato Alkyl Oxetanes*. Patent US 5214166, **1993**.
[20] Biedron, T.; Kubisa, P.; Penczek, S. Polyepichlorohydrin Diols Free of Cyclics: Synthesis and Characterization. *J. Polym. Sci. Part A Polym. Chem.* **1991**, *29*(5): 619-628.
[21] Barbieri, U.; Keicher, T.; Polacco, G. Homo- and Copolymers of 3-Tosyloxymethyl-3-methyl Oxetane (TMMO) as Precursors to Energetic Azido Polymers. *E-Polym.* **2009**, *9*(1): 565-575.
[22] Liu, Z. R. *Thermal Analyses for Energetic Materials*. 1st ed., National Defense Industry Press, Beijing/China **2008**, pp. 22; ISBN 978-7-118-05972-4.
[23] Mo, H. C.; Lu, X. M.; Li, N.; Xing, Y.; Han, T.; Li, L.; Zhang, Z. G. Synthesis and Characterization of Copolyether of 3-Nitratomethyl-3-methyloxetane and Tetrahydrofuran. (in Chinese) *Chin. J. Energ. Mater.* **2012**, *20*(2): 172-175.
[24] Mo, H. C.; Gan, X. X. Synthesis and Properties of 3-Nitratomethyl-3-ethyloxetane and Its Homopolymer. (in Chinese) *Chin. J. Energ. Mater.* **2007**, *15*(4): 313-315,319.
[25] Oyumi, Y.; Brill, T. B. Thermal Decomposition of Energetic Materials 14. Selective Product Distributions Evidenced in Rapid, Real-time Thermolysis of Nitrate Esters

at Various Pressures. *Combust. Flame* **1986**, *66*(1): 9-16.

[26] Oyumi, Y.; Brill, T. B. Thermal Decomposition of Energetic Materials 22. The Contrasting Effects of Pressure on the High-rate Thermolysis of 34 Energetic Compounds. *Combust. Flame* **1987**, *68*(2): 209-216.